Bitmap Algorithms for Counting Active Flows on High-Speed Links

Cristian Estan, George Varghese, *Member, IEEE*, and Michael Fisk

***Abstract*—This paper presents a family of bitmap algorithms that address the problem of counting the number of distinct header patterns (flows) seen on a high-speed link. Such counting can be used to detect DoS attacks and port scans and to solve measurement problems. Counting is especially hard when processing must be done within a packet arrival time (8 ns at OC-768 speeds) and, hence, may perform only a small number of accesses to limited, fast memory. A naive solution that maintains a hash table requires several megabytes because the number of flows can be above a million. By contrast, our new probabilistic algorithms use little memory and are fast. The reduction in memory is particularly important for applications that run multiple concurrent counting instances. For example, we replaced the port-scan detection component of the popular intrusion detection system Snort with one of our new algorithms. This reduced memory usage on a ten minute trace from 50 to 5.6 MB while maintaining a 99.77% probability of alarming on a scan within 6 s of when the large-memory algorithm would. The best known prior algorithm (probabilistic counting) takes four times more memory on port scan detection and eight times more on a measurement application. This is possible because our algorithms can be customized to take advantage of special features such as a large number of instances that have very small counts or prior knowledge of the likely range of the count.**

***Index Terms*—Counting distinct elements, traffic measurements.**

I. Introduction

INTERNET links operate at high speeds, and past trends predict that these speeds will continue to increase rapidly. Routers and intrusion detection devices that operate at up to OC-768 speeds (40 Gb/s) are currently being developed. While the main bottlenecks (e.g., lookups, classification, and quality of service) in a traditional router are well understood, what are the corresponding functions that should be hardwired in the brave new world of security and measurement? Ideally, we wish to abstract out functions that are common to several security and measurement applications and find efficient algorithms for these functions, especially algorithms with a compact hardware implementation.

Toward this goal, this paper isolates and provides solutions for an important problem that occurs in various networking applications: counting the number of active flows among packets received on a link during a specified period of time. A flow is defined by a set of header fields; two packets belong to distinct flows if they have different values for the specified header fields that define the flow. For example, if we define a flow by source and destination IP addresses, we can count the number of distinct source–destination IP address pairs seen on a link over a given time period. Our algorithms measure the number of active flows using a very small amount of memory that can easily be stored in on-chip SRAM or even processor registers. By contrast, naive algorithms described below would require massive amounts of memory necessitating the use of slow DRAM.

For example, a naive method to count source–destination pairs would be to keep a counter together with a hash table that stores all the distinct 64-bit source destination address pairs seen thus far. When a packet arrives with source and destination addresses say $\langle S, D\rangle$, we search the hash table for $\langle S, D\rangle$; if there is no match, the counter is incremented and $\langle S, D\rangle$ is added to the hash table. Unfortunately, given that backbone links can have up to a million flows [7] today, this naive scheme would minimally require 64 Mb of high-speed memory.[1] Such large SRAM memory is expensive or not feasible for a modern router.

There are more efficient general-purpose algorithms for counting the number of distinct values in a multiset. In this paper, we not only present a general-purpose counting algorithm—multiresolution bitmap—that has better accuracy than the best known prior algorithm, probabilistic counting [8], but introduce a whole family of counting algorithms that further improve performance by taking advantage of particularities of the specific counting application. Our adaptive bitmap, using the fact that the number of active flows does not change very rapidly, can count the number of distinct flows on a link that contains anywhere from 0 to 100 million flows with an average error of less than 1% using only 2 kB of memory. Our triggered bitmap, which is optimized for running multiple concurrent instances of the counting problem, many of which have small counts, is suitable for detecting port scans and uses even less memory than running adaptive bitmap on each instance.

A. Problem Statement

A flow is defined by an identifier given by the values of certain header fields.[2] The problem we wish to solve is counting the number of distinct flow identifiers (flow IDs) seen in a specified measurement interval. For example, an intrusion detection system looking for port scans could count for each active source

Manuscript received February 12, 2004; revised August 4, 2005; approved by IEEE/ACM Transactions on Networking Editor M. Crovella. This work was supported in part by the National Science Foundation under Grant ANI-0137102 and by the National Institutes of Standards and Technology Sensilla Project under NIST Grant 60NANB1D0118.

C. Estan is with the Department of Computer Sciences, University of Wisconsin-Madison, Madison, WI 53706 USA (e-mail: estan@cs.wisc.edu).

G. Varghese and M. Fisk are with the Department of Computer Science and Engineering, University of California at San Diego, La Jolla, CA 92093 USA (e-mail: varghese@cs.ucsd.edu; mfisk@cs.ucsd.edu).

Digital Object Identifier 10.1109/TNET.2006.882836

[1] It must at least store the flow identifier, which in this example is 64 bits, for each of a million flows.

[2] We can also generalize by allowing the identifier to be a function of the header fields (e.g., using prefixes instead of addresses, based on routing tables).

address the flows defined by destination IP and port and suspect any source IP that opens more than three flows in 12 s of scanning.

Also, while many applications define flows at the granularity of TCP connections, one may want to use other definitions. For example, when detecting DoS attacks we may wish to count the number of distinct sources, not the number of TCP connections. Thus, in this paper, we use the term flow in this more generic way.

As we have seen, a naive solution using a hash table of flow IDs is accurate but takes too much memory. In high-speed routers, it is not only the cost of large, fast memories that is a problem but also their power consumption and the board space they take up on line cards. Thus, we seek solutions that use a small amount of memory and have high accuracy. Usually, there is a tradeoff between memory usage and accuracy. We want to find algorithms where these tradeoffs are favorable. Also, since at high speeds the per-packet processing time is limited, it is important that the algorithms use few memory accesses per packet. We describe algorithms that use only one or two memory accesses[3] and are simple enough to be implemented in hardware.

B. Motivation

Why is information about the number of flows useful? We describe four possible categories of use.

Detecting port scans: Intrusion detection systems warn of port scans when a source opens too many connections within a given time.[4] The widely deployed Snort intrusion detection system (IDS) [19] uses the naive approach of storing a record for each active connection. This is an obvious waste since most of the connections are not part of a port scan. Even for actual port scans, if the IDS only reports the number of connections, we do not need to keep a record for each connection. Since the number of sources can be very high, it is desirable to find algorithms that count the number of connections of each source using little memory. Further, if an algorithm can distinguish quickly between suspected port scanners and normal traffic, the IDS need not perform expensive operations (e.g., logging) on most of the traffic, thus becoming more scalable in terms of memory usage and speed. This is particularly important in the context of the recent race to provide wire-speed intrusion detection [1].

Detecting denial of service (DoS) attacks: FlowScan by Plonka [18] is a popular tool for visualizing network traffic. It uses the number of active flows (see Fig. 1) to detect ongoing denial of service attacks. While this works well at the edge of the network (i.e., the link between a large university campus and the rest of the Internet), it does not scale to the core. Also, it relies on massive intermediate data (NetFlow) to compute compact results—could we obtain the useful information more directly? Mahajan *et al.* propose a mechanism that allows backbone routers to limit the effect of (distributed) DoS attacks [13]. While the mechanism assumes that these routers can detect an ongoing attack it does not give a concrete algorithm for it. Estan and Varghese present algorithms that can detect destination addresses or prefixes that receive large amounts of traffic [4]. While these can identify the victims of attacks, it also gives many false positives because many destinations have large amounts of legitimate traffic. To differentiate between legitimate traffic and an attack, we can use the fact that DoS tools use fake source addresses chosen at random.[5] If for each suspected victim we count the number of sources of packets that come from some networks known to be sparsely populated, a large count is a strong indication that a DoS attack is in progress.

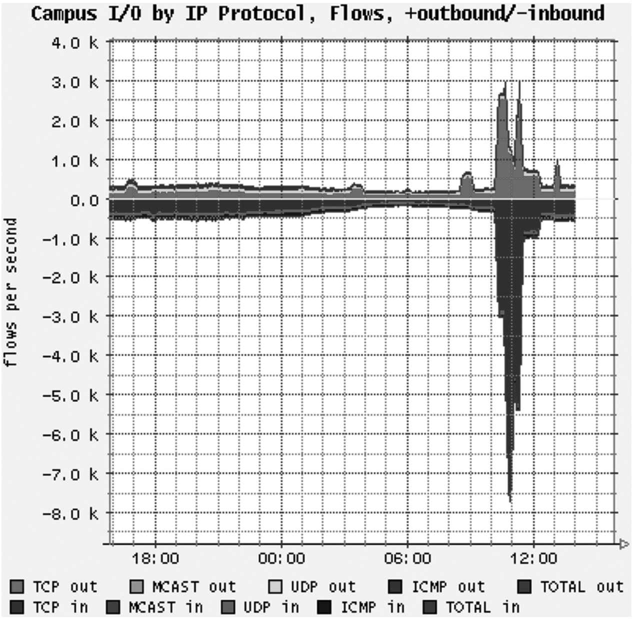

Fig. 1. Flow count provided by Plonka's FlowScan is used to detect DoS attacks.

General measurement: Counting the number of active connections and the number of connections associated with each source and destination IP address is part of the CoralReef [11] traffic analysis suite. Other ways of counting distinct values in given header fields can also provide useful data. One could measure the number of sources using a protocol version or variant to get an accurate image of protocol deployment. Alternatively, by counting the number of connections associated with each of the protocols generating significant traffic, we can compute the average connection length for each protocol, thus getting a better view of its behavior. Dimensioning the various caches in routers (packet classification caches, multicast route caches for source–group (S-G) state, and ARP caches) also benefits from prior measurements of typical workload.

Estimating the spreading rate of a worm: From August 1 to August 12, 2001, while trying to track the Code Red worm [15], collecting packet headers for Code Red traffic on a /8 network produced 0.5 GB per hour of compressed data. To determine the rate at which the worm was spreading, it was necessary to

[3] Larger numbers of memory accesses are feasible at high speeds using SRAM and pipelining, but this increases the cost of the solution.

[4] While distributed port scans are possible, they are harder because the attacker has to control many endhosts from which it can scan. If the number of hosts is not very large, each will have to probe many port–destination combinations thus running the risk of being detected.

[5] If the attack uses few source addresses, it can be easily filtered out once those addresses are identified. Identifying those addresses can be done using previous techniques [4], because those few source addresses must send a lot of traffic each for the attack to be effective.

count the number of distinct Code Red sources passing through the link. This was actually done using a large log and a hash table which was expensive in time and also inaccurate (because of losses in the log).

Thus, while counting the number of flows is usually insufficient by itself, it can provide a useful building block for complex tasks. This paper extends an earlier conference version [5]. The most important additions are a discussion of hardware implementations of the bitmap counting algorithms, a detailed discussion of the similarities and differences between our multiresolution bitmap and probabilistic counting, and a discussion of more recent related work.

II. Related Work

The networking problem of counting the number of distinct flows has a well-studied equivalent in the database community: counting the number of distinct database records (or distinct values of an attribute). Thus, the major piece of related work is a seminal algorithm, *probabilistic counting*, due to Flajolet and Martin [8], introduced in the context of databases. We use probabilistic counting as a base against which to compare our algorithms. Whang *et al.* address the same problem and propose an algorithm [22] equivalent to the simplest algorithm we describe (direct bitmap).

The insight behind probabilistic counting is to compute a metric of how uncommon a certain record is and keep track of the most uncommon records seen. If the algorithm sees very uncommon records, it concludes that the number of records is large. More precisely, for each record, the algorithm computes a hash function that maps it to an L bit string (L is configurable). It then counts the number of consecutive zeroes starting from the least significant position of the hash result and sets the corresponding bit in a bitmap of size L. If the algorithm sees records that hash to values ending in zero, one, and two 0's (the first three bits in the bitmap are set, and the rest are not), it concludes that the number of distinct records was $c \cdot 2^2$ (c is a statistical correction factor). If it also sees hash values ending in three 0's, it estimates $c \cdot 2^3$ and so on. This basic form can have an accuracy of at most 50% because possible estimates are a factor of two from each other. Probabilistic counting divides the hash values into $nmap$ groups ($nmap$ is configurable), runs a separate instance of the basic algorithm for each group, and averages over the estimates for the count provided by each of them, thus reducing the error of its final estimate. Durand and Flajolet have recently proposed [14] a variant of probabilistic counting with better asymptotic memory usage. We describe a family of algorithms that each outperforms probabilistic counting by an order of magnitude by exploiting application-specific characteristics.

In networking, there are general-purpose traffic measurement systems such as Cisco's NetFlow [16] or LFAP [17] that report per-flow records for very fine-grained flows. This is useful for traffic measurement and can be used to count flows (and this is what FlowScan [18] does), but is not optimized for such a purpose. Besides the large amount of memory needed, in modern high-speed routers, updating state on every packet arrival is infeasible at high speeds. Ideally, such state should be in high-speed SRAM (which is expensive and limited) to allow wire-speed forwarding.

Because the NetFlow state is so large, Cisco routers write NetFlow state to slower DRAM which slows down packet processing. For high speeds, sampling needs to be turned on: only the sampled packets result in updates to the flow cache that keeps the per flow state. Unfortunately, sampling has problems of its own since it affects the accuracy of the measurement data. Sampling works reasonably for estimating the traffic sent by large flows or large traffic aggregates, but has extremely poor accuracy for estimating the number of flows. This is because uniform sampling produces more samples of flows that send more traffic, thereby biasing any simple estimator that counts the number of flows in the sample and applies a correction.

Duffield *et al.* present two scalable methods for counting the number of active TCP flows based on samples of the traffic [2]. They rely on the fact that TCP turns the SYN flag on only for the packets starting a connection. The estimates are based on counts of the number of flows with SYN packets in the sampled data. While this is a good solution for TCP connections, it cannot be applied to UDP or when we use a different definition for flows (e.g., when looking at protocol deployment statistics, we define a flow as all packets with the same source IP). Also, counting flows in the sampled data can still be a memory-consuming operation that needs to be efficiently implemented.

The Snort [19] IDS uses a memory-intensive approach similar to NetFlow to detect port scans: it maintains a record for each active connection and a connection counter for each source IP. This problem is solved more efficiently by the triggered bitmaps proposed here. Venkataraman *et al.* [21] and Keys *et al.* [10] propose even more memory-efficient solutions to the same problem. Kumar *et al.* [12] have used multiresolution techniques similar to our multiresolution bitmap to solve the related but different problem of counting packets in a flow.

III. A Family of Counting Algorithms

Our family of algorithms for estimating the number of active flows relies on updating a bitmap at run time. Different members of the family have different rules for updating the bitmap. At the end of the measurement interval (1 second, 1 minute, or even 1 hour), the bitmap is processed to yield an estimate for the number of active flows. Since we do not keep per-flow state, all of our results are estimates. However, we prove analytically and show through experiments on traces that our estimates are close to actual values. The family contains three core algorithms and three derived algorithms. Even though the first two core algorithms (direct and virtual bitmap) were invented previously, we present them here because they form the basis of our new algorithms (multiresolution, adaptive, and triggered bitmaps), and because we present new applications in a networking context (as opposed to a database or wireless context).

We start in Section III-A with the first core algorithm *direct bitmap* that uses a large amount of memory. Next, in Section III-B, we present the second core algorithm called *virtual bitmap* that uses sampling over the flow ID space to reduce the memory requirements. While virtual bitmap is extremely accurate, it needs to be tuned for a given anticipated range of the number of flows. We remove the "tuning" restriction of virtual bitmap with our third algorithm called *multiresolution bitmap*, described in Section III-C, at the cost of increased memory usage. Finally, in Section III-D, we describe the two derived algorithms. In this section, we only describe the algorithms; we leave an analysis of the algorithms to Section IV. Our algorithms are implemented by the publicly available bmpcount library [3].

A. Direct Bitmap

The direct bitmap is a simple algorithm for estimating the number of flows. We use a hash function on the flow ID to map each flow to a bit of the bitmap. At the beginning of the measurement interval all bits are set to zero. Whenever a packet comes in, the bit its flow ID hashes to is set to 1. Note that all packets belonging to the same flow map to the same bit, so each flow turns on at most one bit irrespective of the number of packets it sends.

We could use the number of bits set as our estimate of the number of flows, but this is inaccurate because two or more flows can hash to the same bit. In Section IV-A, we derive a more accurate estimate that takes into account hash "collisions."[6] Even with this better estimate, the algorithm becomes very inaccurate when the number of flows is much larger than the number of bits in the bitmap and the bitmap is almost full. The only way to preserve accuracy is to have a bitmap size that scales almost linearly with the number of flows, which is often impractical.

B. Virtual Bitmap

The virtual bitmap algorithm reduces the memory usage by storing only a small portion of the big direct bitmap one would need for accurate results (see Fig. 2) and extrapolating the number of bits set. This can also be thought of as sampling the flow ID space. The larger the number of flows, the smaller the portion of the flow ID space we cover. Virtual bitmap generalizes direct bitmap: direct bitmap is a virtual bitmap which covers the entire flow ID space.

Unfortunately, a virtual bitmap does require tuning the "sampling factor" based on prior knowledge of the number of flows. If it differs significantly from what we configured the virtual bitmap for, the estimates are inaccurate. If the number of flows is too large the virtual bitmap fills up and has the same accuracy problems as an underdimensioned direct bitmap. If the number of flows is too small we have another problem: say the virtual bitmap covers 1% of the flow ID space and there are 50 active flows—if none of them hashes to the virtual bitmap, the algorithm will suppose the number of flows is 0, if 1 hashes, the algorithm will estimate 100, but it will never estimate 50. The optimal sampling factor obtains the best tradeoff between "collision errors" and "extrapolation errors."

While, in general, one wants an algorithm that is accurate over a wider range, we note that even an unadorned virtual bitmap is useful. For example, a security application may wish to trigger an alarm when the number of flows crosses a threshold. The virtual bitmap can be tuned for this threshold and uses less memory than other algorithms that are accurate not just around the threshold, but over a wider range for the number of flows.

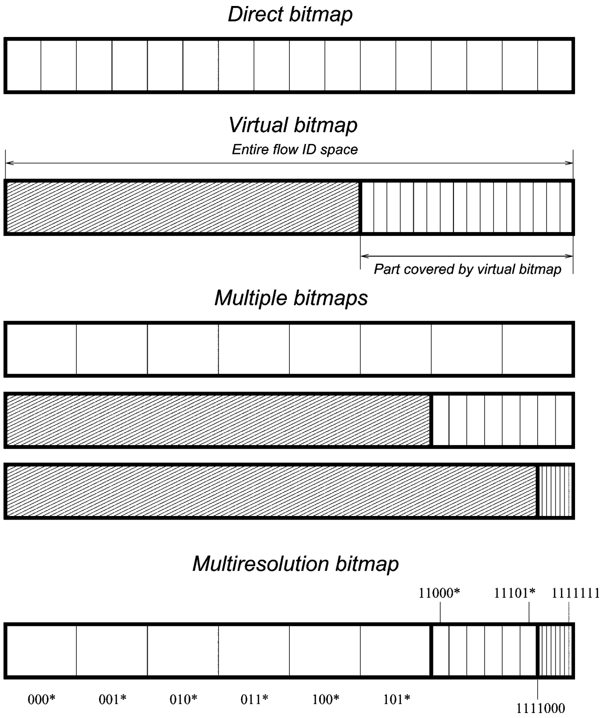

Fig. 2. Multiresolution bitmap from this example uses a single 7-bit hash function to decide which bit to map a flow to. It gives results as accurate as the three virtual bitmaps, thus covering a wide range for the number of flows, but it performs a single memory update per packet. Note that all of the unfilled "tiles" from these bitmaps, despite their different sizes, represent one bit of memory.

In Section IV, we derive formulas for the average error of the virtual bitmap estimates. The analysis also provides insight for choosing the right sampling factor. Perhaps surprisingly, the analysis also indicates that the average error depends only on the number of bits and not on the number of flows as long as the sampling factor is set to an optimal value (e.g., with 215 B, the average error is 3%).

C. Multiresolution Bitmap

The virtual bitmap is simple to implement, uses little memory, and gives very accurate results, but requires us to know in advance a reasonably narrow range for the number of flows. An immediate solution to this shortcoming is to use many virtual bitmaps, each using the same number of bits of memory, but different sampling factors, so that each is accurate for a different range of the number of active flows (different "resolutions"). The union of all of these ranges is chosen to cover all possible values for the number of flows. When we compute our estimate, we use the virtual bitmap that is most accurate based on a simple rule that looks at the number of bits set. The "lowest resolution" bitmap is a direct bitmap that works well when there are very few flows. The "higher resolution" bitmaps cover a smaller and smaller portions of the flow ID space and work well when the number of flows is larger. The problem with the naive approach of using several virtual bitmaps is that instead of updating one bitmap for each packet, we need to update several, causing more memory accesses.

[6] We assume in our analysis that the hash function distributes the flows randomly. In an adversarial setting, the attacker who knows the hash function could produce flow identifiers that produce excessive collisions thus evading detection. This is not possible if we use a random seed to our hash function.

The main innovation in multiresolution bitmap is to maintain the advantages of multiple bitmaps configured for various ranges while performing a *single update* for each incoming packet. Fig. 2 illustrates the direct bitmap, virtual bitmap, multiple bitmaps, and multiresolution bitmap. Before explaining how the multiresolution bitmap works, it can help to switch to another way of thinking about how the virtual bitmap operates. We can consider that, instead of generating an integer, the hash function covers a continuous interval. The virtual bitmap covers a portion of this interval (the ratio of the sizes of the interval covered by the virtual bitmap and the entire interval is the sampling factor of the virtual bitmap). We divide the interval corresponding to the virtual bitmap into equal sized subintervals, each corresponding to a bit. A bit in the virtual bitmap is set to 1 if the hash of the incoming packet maps to the subinterval corresponding to the bit. The multiple bitmaps solution is shown below the virtual bitmap solution in Fig. 2.

A multiresolution bitmap is essentially a combination of multiple bitmaps of different "resolutions" such that a single hash is computed for each packet and only the highest resolution bitmap it maps to is updated. Thus, each bitmap loses a portion of its bits which are covered by higher resolution bitmaps. We call these regions with different resolutions components of the multiresolution bitmap. When computing the estimate, based on the number of bits set in each component, we choose one of them as "base," estimate the number of flows hashing to it and all finer components, and extrapolate. For example, if the leftmost 6-bit matching keys 000* to 101* in Fig. 2 are set, they will not be used. Instead, we can choose as base the next component and, based on the six bits in the next component and the eight in the last one, estimate the number of flows hashing to the last quarter of the hash space (11^*) and estimate the total number of flows by multiplying this number by four.

In Section IV-C, we answer questions such as: how many bits should each component have, how many components do we need, and what is the best ratio between the resolutions of neighboring components? In Appendix A, we show that multiresolution bitmaps are easy to implement even in hardware. In Appendix B, we compare our multiresolution bitmap to probabilistic counting, showing that, while both algorithms use statistically equivalent hashes to set bits, they interpret the data *very* differently, thus the differences in the accuracy of the results.

D. Derived Algorithms

Here, we describe two derived algorithms for counting active flows. *Adaptive bitmap*, described Section III-D1, achieves both the accuracy of virtual bitmap and the robustness of multiresolution bitmap by combining them and relying on the stationarity of the number of flows. *Triggered bitmap*, which is described in Section III-D2, combines direct bitmap and multiresolution bitmap to reduce the total amount of memory used by multiple instances of flow counting when most of the instances count few flows.

1) Adaptive Bitmap: Can we build an algorithm that provides the best of both worlds: the accuracy of a well tuned virtual bitmap with the wide range of multiresolution bitmaps? Adaptive bitmap is such an algorithm that combines a large virtual bitmap and a small multiresolution bitmap. It relies on a simple observation: measurements show that the number of active flows does not change dramatically from one measurement interval to the other (so it is not suitable for tracking say attacks where sudden changes are expected). We use the small multiresolution bitmap to detect changes in the order of magnitude of the count and the virtual bitmap for precise counting within the currently expected range. The number of flows we expect is the number of flows measured in the previous measurement interval. Assuming "quasi-stationarity," the algorithm is accurate most of the time because it uses the large, well-tuned virtual bitmap for estimating the number of flows. At startup and in the unlikely case of dramatic changes in the number of active flows the multiresolution bitmap provides a less accurate estimate.

Updating these two bitmaps separately would require *two* memory updates per packet, but we can avoid the need for multiple updates by combining the two bitmaps into one. Specifically, we use a multiresolution bitmap in which r adjacent components are replaced by a single large component consisting of a virtual bitmap (where r is a configuration parameter). The location of the virtual bitmap within the multiresolution bitmap (i.e., which components it replaces) is determined by the current estimate of the count. If the current number of flows is small, we replace coarse components with the virtual bitmap. If the number of flows is large, we replace fine components with the virtual bitmap. The update of the bitmap happens exactly as in the case of the multiresolution bitmap, except that the logic is changed slightly when the hash value maps to the virtual bitmap component.

2) Triggered Bitmap: Consider the concrete example of detecting port scans. If one used a multiresolution bitmap per active source to count the number of connections, the multiresolution bitmap would need to be able to handle a large number of connections because port scans can use very many connections. The size of such a multiresolution bitmap can be quite large. However, most of the traffic is not port scans and most sources open only one or two connections. Thus, using a large bitmap for each source is wasteful.

The triggered bitmap combines a very small direct bitmap with a large multiresolution bitmap. All sources are allocated a small direct bitmap. Once the number of bits set in the small direct bitmap exceeds a certain trigger value, a large multiresolution bitmap is allocated for that source and it is used for counting the connections from there on. Our estimate for the number of connections is the sum of the flows counted by the small direct bitmap and the multiresolution bitmap. This way, we have accurate results for all sources but only pay the cost of a large multiresolution bitmap for sources with many connections.

As described so far, this algorithm introduces a subtle error that makes a small change necessary. If a flow is active both before and after the large multiresolution bitmap is allocated it gets counted by both the direct bitmap and the multiresolution bitmap. Only using the multiresolution bitmap for our final estimate is not a solution either because we would not count the flows that were active only before the multiresolution bitmap was allocated. To avoid this problem, we change the algorithm the following way: after the multiresolution bitmap is allocated, we only map to it flows that do not map to one of the bits already set in the direct bitmap. This way, if the flows that set the bits in the direct bitmap send more packets, they will not influence the multiresolution bitmap. It is true that the multiresolution bitmap does not catch all the new flows, just the ones that map to one of the bits not set in the direct bitmap. This is equivalent to the "sampling factor" of the virtual bitmap and we can compensate for it (see Section IV-A).

IV. Algorithm Analysis

Here, we provide the analyses of the statistical behavior of the bitmaps used by our algorithms. We focus on three types of results. In Section IV-A, we derive formulas for estimating the number of active flows based on the observed bitmaps. In Section IV-B, we analytically characterize the accuracy of the algorithms by deriving formulas for the average error of the estimates. In Section IV-C, we use the analysis to derive rules for dimensioning the various bitmaps so that we achieve the desired accuracy over the desired range for the number of flows.

A. Estimate Formulas

Direct bitmap: To derive a formula for estimating the number of active flows for a direct bitmap, we have to take into account collisions. Let b be the size of the bitmap. The probability that a given flow hashes to a given bit is $p = 1/b$. Assuming that n is the number of active flows, the probability that no flow hashes to a given bit is $p_z = (1-p)^n \approx (1/e)^{n/b}$. By linearity of expectation, this formula gives us the expected number of bits not set at the end of the measurement interval $E[z] = bp_z \approx b(1/e)^{n/b}$. If the number of zero bits is z, (1) gives our estimate $\widehat{n}$ for the number of active flows. Whang *et al.* also show that this is the maximum-likelihood estimator for the number of active flows [22]

$$\widehat{n} = b \ln\left(\frac{b}{z}\right). \tag{1}$$

Virtual bitmap: Let α be the "sampling factor" (the ratio of the sizes of the interval covered by the virtual bitmap b and the entire hash space h). The probability for a given flow to hash to the virtual bitmap is equal to the sampling factor $p_v = \alpha = b/h$. Let m be the number of flows that actually hash to the virtual bitmap. Its probability distribution is binomial with an expected value of $E[m] = \alpha n$. We can use (1) to estimate m and, based on that, we obtain

$$\widehat{n} = \frac{1}{\alpha} b \ln\left(\frac{b}{z}\right) = h \ln\left(\frac{b}{z}\right) \tag{2}$$

for the estimate of the number of active flows n.

Multiresolution bitmap: The multiresolution bitmap is a combination of c components, each tuned to provide accurate estimates over a particular range. When we compute our estimate we do not know in advance which component is the one that provides the most accurate estimate (we call this the base component). As we will see in Section IV-B, we obtain the smallest error by choosing as the base component the coarsest component that has no more than $set_{\max}$ bits (lines 1–5 in Fig. 3). $set_{\max}$ is a precomputed threshold based on the analysis from Section IV-B. Once we have the base component, we estimate the number of flows m hashing to the base and all the higher resolution ones using (1) and add them together (lines 13–17 in Fig. 3). To obtain the result, we only need to perform the multiplication corresponding to the sampling factor (lines 18 and 19). Other parameters used by this algorithm are the ratio k between the resolutions of neighboring components and b_{last} the number of bits in the last component (which is different from b).

```
ESTIMATEFLOWCOUNT
1   $base = c - 1$
2   while $base > 0$ and $bitsSet(component[base]) \le set_{max}$
3       $base = base - 1$
4   endwhile
5   $base = base + 1$
6   if $base == c$ and $bitsSet(component[c]) > setlast_{max})$
7       if $bitsSet(component[c]) == b_{last}$
8           return "Cannot give estimate"
9       else
10          warning "Estimate might be inaccurate"
11      endif
12  endif
13  $m = 0$
14  for $i = base$ to $c - 1$
15      $m = m + b\ln(b/bitsZero(component[i]))$
16  endfor
17  $m = m + b_{last}\ln(b_{last}/bitsZero(component[c]))$
18  $factor = k^{base-1}$
19  return $factor * m$
```

Fig. 3. Algorithm for computing the estimate of the number of active flows for a multiresolution bitmap. We first pick the base component that gives the best accuracy then add the estimates for the number of flows hashing to it and higher resolution components and finally extrapolate.

Adaptive bitmap: The algorithm for adaptive bitmap is very similar to multiresolution bitmap. The main difference is that we use different threshold for selecting the big component as base. For brevity, we omit the algorithm.

Triggered bitmap: If the triggered bitmap did not allocate a multiresolution bitmap, we simply use the formula for direct bitmaps [see (1)]. Let us use g for the number of bits that have to be set in the direct bitmap before the multiresolution bitmap is allocated and d for the total number of bits in the direct bitmap. If the multiresolution bitmap is deployed, we use the algorithm from Fig. 3 to compute the number of flows hashing to the multiresolution bitmap, multiply that by $d/(d-g)$ and add the estimate of the direct bitmap.

B. Accuracy

To determine the accuracy of these algorithms, we look at the standard error of our estimate $\widehat{n}$, that is, the standard deviation of the ratio $\widehat{n}/n$. We also refer to this quantity as the average (relative) error $SD[\widehat{n}/n] = SD[\widehat{n}]/n$. One parameter that is useful in these analyses is the flow density ρ, which is defined as the average number of flows that hash to a bit.

Direct bitmap: While our formula for estimating the number of active flows accounts for the expected collisions, it does not always give exact results because the number of collisions is random. Equation (3) approximates the average error of a direct bitmap based on the Taylor expansion of (1) as derived by Whang *et al.* [22]. The result is not exact because because less significant terms of the Taylor expansion were omitted.

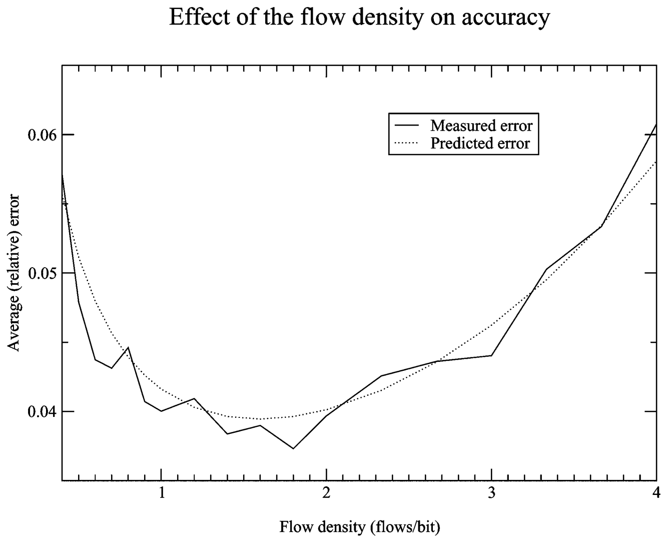

Fig. 4. When the flow density is too low, the “sampling error” takes over; when it is too high, “collision error” is the main factor. We get the best accuracy for a flow density of around $\rho = 1.6$. The estimate from (4) matches well the experimental results being slightly conservative (larger). See Section V-A for details of the experiment.

Whang *et al.* also show that the approximation does not lead to serious inaccuracies for configurations one expects to see in practice. They also show that the distribution of the number of bits set is asymptotically normal, so errors much larger than the standard error are very unlikely [22]. For example, for a direct bitmap configured to operate at an average error of 10% for flow densities up to $\rho = 2$, the value of the average error we get by including the next term of the Taylor series is only 2% away from the approximation (i.e., the actual average error can be at most 10.2% instead of 10%). The inaccuracy introduced by the approximation decreases further as the number of bits increases.

$$SD\left[\frac{\widehat{n}}{n}\right] \approx \frac{\sqrt{e^{\rho} - \rho - 1}}{\rho\sqrt{b}} \tag{3}$$

Virtual bitmap: Besides the randomness in the collisions, there is another source of error for the virtual bitmap: we assume that the ratio between the number of flows that hash to the physical bitmap and all flows is exactly the sampling factor while due to the randomness of the process the number can differ. Detailed analysis of these two errors and how they interact is available [5]. Equation (4) takes into account their cumulative effect on the result. When the flow density is too large, the error increases exponentially because of the collision errors. When it is too small, the error increases as the sampling errors take over. Our analysis also shows that the terms ignored by the approximations do not contribute significantly and that the bound is tight. Fig. 4 presents a typical result comparing the measured average error from simulations on traces of actual traffic with the value from

$$SD\left[\frac{\widehat{n}}{n}\right] \lessapprox \frac{\sqrt{e^{\rho} - 1}}{\rho\sqrt{b}}. \tag{4}$$

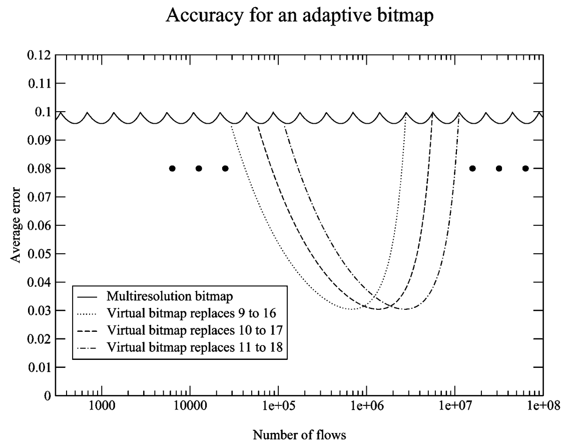

Fig. 5. Large virtual bitmap replaces six of the components of the multiresolution bitmap. The size of the normal components is $b = 64$ bits and the size of the large virtual bitmap is $v = 1627$ bits. The adaptive bitmap guarantees an average error of at most 10% over the whole range, but if the number of flows falls into the “sweet spot” the average error can be as low as 3.1%.

Multiresolution bitmap: To compute the average error of the estimate of the multiresolution bitmap, we should take into account separately the collision errors of all components finer than the base. This would result for a different formula for each component that would be used as base. Equation (5) is a slightly weaker bound that holds for all components but the last one as long as the number of bits in the last component b_{last} is large enough [3]. Equation (5) bounds quite tightly the average error for a normal component. For the last component of the multiresolution bitmap, we use (4) directly to yield

$$SD\left[\frac{\widehat{n}}{n}\right] \lessapprox \frac{\sqrt{\frac{k-1}{k}\left(e^{\rho} + e^{\rho/k} - 2\right) + e^{\rho/k^2} - 1}}{\rho\sqrt{\frac{bk}{k-1}}}. \tag{5}$$

Adaptive bitmap: The error of the estimates of the adaptive bitmap depends strongly on the number of flows: the errors are much larger if the number of flows is unexpectedly large or small. The exact formulas, which are omitted here for brevity, are not very different from the ones seen so far. We give an example instead. Fig. 5 gives the average error as predicted by our formulas for the adaptive bitmap we use in for measurements (Section V-C). We first represent the average error of the original multiresolution bitmap and then the average error we obtain by replacing various groups of eight consecutive components with the virtual bitmap. It is apparent from this figure that, by changing which components are replaced by the virtual bitmap, we can change the range for which the adaptive bitmap is accurate.

C. Configuring the Bitmaps

Here, we address the configuration details and implicitly the memory needs of the bitmap algorithms. The publicly available library implementing the bitmap algorithms described in this paper [3] also has scripts implementing the numerical computations for configuring them, discussed in this section. The two

TABLE I
THE USER SPECIFIES AN ACCEPTABLE RELATIVE ERROR ϵ AND A MAXIMUM NUMBER OF FLOWS TO COUNT N WITH THE GIVEN ERROR (FOR VIRTUAL BITMAP, N IS THE NUMBER OF FLOWS FOR WHICH MAXIMUM ACCURACY IS ACHIEVED). BASED ON THESE NUMBERS, ONE CAN COMPUTE THE CONFIGURATION PARAMETERS WHICH ALSO DETERMINE THE AMOUNT OF MEMORY REQUIRED. USING $k = 2$ GIVES LOW MEMORY USAGE, AND THE VALUES OF 3 AND 4 ONLY RARELY RESULT IN SLIGHTLY LOWER MEMORY

Algorithm	Memory (bits)	Parameters
Direct bitmap	$< N/\ln(N\epsilon^2 + 1)$	b
Virtual bitmap	$1.544/\epsilon^2$	b, α
Multires. bmp.	$0.919 \ln(N\epsilon^2)/\epsilon^2 + ct.$	b, c, k, b_{last}
Adaptive bmp.	$\gtrapprox 1.544/\epsilon^2$	b, c, k, b_{last}, v

TABLE II
THE THRESHOLD $set_{\max}$ USED TO DECIDE WHICH COMPONENT TO USE IS PROPORTIONAL TO THE COMPONENT SIZE $b = f(k)/\epsilon^2$ WHICH DEPENDS ON THE DESIRED ACCURACY. $f(k)/\ln(k)$ IS THE ASYMPTOTIC MEMORY USAGE FOR VARIOUS VALUES FOR THE RATIO BETWEEN RESOLUTIONS OF NEIGHBORING COMPONENTS k

k	set_{max}/b	coefficient $f(k)$	$f(k)/\ln(k)$
2	0.9311	0.6367	0.9186
3	0.9463	1.0318	0.9392
4	0.9568	1.3470	0.9717

TABLE III
AS WE INCREASE THE NUMBER OF COMPONENTS r REPLACED BY THE VIRTUAL BITMAP, THE SIZE OF THE VIRTUAL BITMAP v ALMOST DOUBLES FOR EACH NEW COMPONENT REPLACED. THE RATIO BETWEEN THE AVERAGE ERROR OF THE LARGE VIRTUAL BITMAP AND THE MULTIRESOLUTION BITMAP ALSO INCREASES, BUT AT A SLOWER RATE THAN THE SIZE OF THE VIRTUAL BITMAP

r	v/b	improvement
2	2.3626	1.1725
3	4.4861	1.4488
4	8.0603	1.8468
5	14.3252	2.4029
6	25.5510	3.1709
7	45.9411	4.2265
8	83.3330	5.6754
9	152.4217	7.6641
10	280.8654	10.3959
11	520.9068	14.1524
12	971.5300	19.3240

main parameters we use to configure the bitmaps are the maximum number of flows one wants them to count N and the acceptable average *relative* error ϵ. We base our computations on the formulas of the previous section.

Direct bitmap: If we would keep $\rho = N/b$ constant as N increased, ϵ would improve proportionally to $1/\sqrt{N}$ (which is proportional to $1/\sqrt{b}$). So, as N increases, the flow density that gives us the desired accuracy also increases. Therefore, by ignoring the constant term under the square root in (3), we get a tight bound on how b scales. $\epsilon^2 \lessapprox (e^\rho - \rho)/(\rho^2 b)$, so $\epsilon^2 N + 1 \lessapprox e^\rho/\rho < e^\rho$. From here, $\rho > \ln(\epsilon^2 N + 1)$ and thus $b < N/\ln(\epsilon^2 N + 1)$. We claim that, for large values of N, while this closed form bound is not tight, it is not very far off either. For example, for $N = 1\,000\,000$ and $\epsilon = 10\%$, the bound gives 108 572 bits, while the actual value is 85 711 bits. Of course, for configuring a direct bitmap, we recommend solving (3) numerically for b (with ρ replaced by N/b).

Virtual bitmap: The average error of the virtual bitmap given by (4) is minimized by a certain value of the flow density. Solving numerically, we get $\rho_{\text{optimal}} = 1.594$ and this corresponds to around 20.3% of the bits of the bitmap being not set. By substituting, we obtain the average error for this "sweet spot" flow density $\epsilon \lessapprox 1.243/\sqrt{b}$. By inverting this, we obtain the formula from Table I for the number of bits of physical memory we need to achieve a certain accuracy. When we need to configure the virtual bitmap as a trigger, we set the sampling factor α such that at the threshold the flow density is 1.594. For this application, if we have 155 bits, the average error of our estimate is at most 10% no matter how large the threshold is. If we have 1716, the average error is at most 3%, and if we have 15 442 it is at most 1%. If we want the virtual bitmap to have at most a certain error for a range of flow counts between $N_{\min}$ and $N_{\max}$, we need to solve the problem numerically by finding a $\rho_{\min} < \rho_{\text{optimal}}$ and a $\rho_{\max} > \rho_{\text{optimal}}$ so that $\rho_{\max}/\rho_{\min} = N_{\max}/N_{\min}$ and $\rho_{\min}$ and $\rho_{\max}$ produce the same error. Once we have these values, we can compute the sampling factor for the virtual bitmap and the number of bits.

Multiresolution bitmap: For brevity, we omit the full discussion of the configuration of the multiresolution bitmap since it is available elsewhere [5]. From (5), we get the rule for choosing the size of the bitmap components as $b = f(k)/\epsilon^2$, where the coefficient $f(k)$ depends on k. Table II also gives the coefficients to compute the threshold $set_{\max}$ used by the algorithm (Fig. 3) to select the base component is $set_{\max} = b\,(1 - e^{-\rho_{\max}})$. Given N, the highest number of flows for which the multiresolution bitmap must stay accurate, the number of components is $c = 2 + \lceil log_k(N/(\rho_{\max} b)) \rceil$. For some configurations, by increasing the size of the last component, b_{last}, one can reduce the number of components by one without increasing the total memory required [3]. The ratio $f(k)/\ln(k)$ gives the asymptotic memory usage for a certain choice of k, and we can see from Table II that $k = 2$ is the best choice. For a few configurations, $k = 3$ needs slightly lower memory as it "fits better" N, because the number of components c must be integer. As described in Appendix A, hardware implementation of the multiresolution bitmap is easier if we restrict k and b to powers of two. For a few hardware configurations, $k = 4$ gives slightly lower memory usage.

Adaptive bitmap: For brevity, we omit the detailed discussion of the configuration of the adaptive bitmap. In Table III, we report the costs and benefits of the adaptive bitmap. The first column lists the number r of normal components we replace with the large one. The next column lists the number of bits the large component needs to have (compared to the number of bits of a normal component) to ensure that the adaptive bitmap never has a worse average error than the original multiresolution bitmap. The third column lists the ratio between the average error of multiresolution bitmap and the "sweet spot" average error of the adaptive bitmap. The memory usage reported in Table I is derived based on the observation that most of the memory of the adaptive bitmap is used by the "virtual bitmap" component.

V. MEASUREMENT RESULTS

We group our measurements into four sections corresponding to the four important algorithms presented: virtual bitmap, multiresolution bitmap, adaptive bitmap, and triggered bitmap.

TABLE IV
TRACES USED FOR OUR MEASUREMENTS

Name	No. of flows (min/avg/max)	Length (s)	Encr.
MAG+	93,437 / 98,424 / 105,814	4515	no
MAG	99,264 / 100,105 / 101,038	90	no
COS	17,716 / 18,070 / 18,537	90	yes
IND	1,964 / 2,164 / 2,349	90	yes

Some measurements are geared toward checking the correctness of our theoretical analysis and others toward comparing the performance of our algorithms with probabilistic counting and other existing solutions.

For our experiments, we used three packet traces: an unencrypted one from CAIDA captured on August 6, 2001, on an OC-48 backbone link and two encrypted traces from the MOAT project of NLANR captured on November 11, 2002, on the connection points of two university campuses to the Internet. The unencrypted trace is very long; for some experiments we also used a 90-s slice of the unencrypted trace as a fourth trace. We usually set the measurement interval to 5 s. We chose 5 s because it appears to be a plausible interval someone would use when looking at the number of active flows: it is larger than the round-trip times we can expect in the Internet but not significantly larger than the duration of the shortest flows. In all experiments we defined the flows by the 5-tuple of source and destination IP addresses, ports, and protocol. Table IV gives a summary description of the traces we used. All algorithms used equivalent CRC-based hash functions with random generator functions. Unless otherwise specified, the experiments have been repeated 20 times with different hash functions and the reported average and maximum errors are over the different runs and the different measurement intervals in the trace.

A. Virtual Bitmap

We performed experiments to check the validity of (3) for various configurations on many traces. Fig. 4 shows a typical result. More results can be found in the technical report version of the paper [6]. Our measurements confirm that (3) gives a tight and slightly conservative bound on the average error (conservative in the sense that actual errors are usually somewhat smaller than predicted by the formula). The results also confirm that we get the best average error for a virtual bitmap of a given size when the flow density is around $\rho = 1.6$.

We also compare the average error of the virtual bitmap to probabilistic counting using the same amount of memory for a variety of configurations and traces. Because our major contributions are the remaining schemes, we provide here only one sample result. For the COS trace, using 1716 bits, our analysis predicts an expected error of 3%. The actual average error (computed as the square root of the average of squares) for virtual bitmap is only 2.773% with a maximum of 9.467%. This is not just a further confirmation that (3) gives a tight bound on the average error, but it also shows that errors much larger than the average error are very unlikely. On the other hand, probabilistic counting configured to handle up to 100 000 flows had an average error of 6.731% with a maximum of 27.336%. While this is an unfair comparison in general (virtual bitmap requires knowing in advance the range of final count values so that we can set α to a value that ensures that ρ is close to 1.6), it does fairly indicate our major message: a problem-specific counting method for a specific problem like threshold detection can significantly outperform a one-size-fits-all technique like probabilistic counting.

B. Multiresolution Bitmap

This set of experiments compares the average error of the multiresolution bitmap and probabilistic counting. A meaningful comparison is possible if we compare the two algorithms over the whole range for the number of flows. Since our traces have a pretty constant number of flows, we use a synthetic trace for this experiment. We used the actual packet headers from the MAG+ trace to generate a trace that has a different number of flows in each measurement interval: from 10 to 1 000 000 in increments of 10% with a jitter of 1% added to avoid any possible effects of "synchronizations" with certain series of numbers.

We ran experiments with multiresolution bitmaps tuned to give an average error of 1%, 3%, and 10% for up to 1 000 000 flows and probabilistic counting configured for the same range with the same memory. For each configuration, we had 500 runs with different hash functions.

Fig. 6 shows the results of the experiments. We can see that, in all three experiments, the average error of the multiresolution bitmap is better than predicted for small values, because we have no "sampling error" when the number of flows is small. We explain the periodic "fluctuations" of average error from Fig. 6(a) by occasional incorrect choice of the base component. The peaks correspond to where components are least accurate and hand off to each other. The peaks are more pronounced in this figure than the others because due to the small number of bits in each component, it happens more often that not the best component is used as a base for the estimation. In Fig. 6(b) and especially in Fig. 6(c), there is a visible decrease in the error for the multiresolution bitmap when the number of flows approaches the upper limit. The reason is that the last component is much larger than the normal ones and provides more accurate results.

Probabilistic counting is worse than the multiresolution bitmap, especially for small values. We show in Appendix B that the data collected by the two algorithms are equivalent, so it might be surprising that their accuracies are so different. We attribute the large errors of probabilistic counting for low values to the way it evaluates the collected data. The ability of multiresolution bitmap to be accurate on the low end of the range too can lead to simpler, more robust systems. We attribute the worse error of probabilistic counting for higher values mostly to the suboptimal dimensioning of the algorithm (as recommended in [8]).

C. Adaptive Bitmap

The experiments from this section compare adaptive bitmap and probabilistic counting on all three traces. The results are presented in Table V. All of the algorithms were configured to use 16 kb of memory.

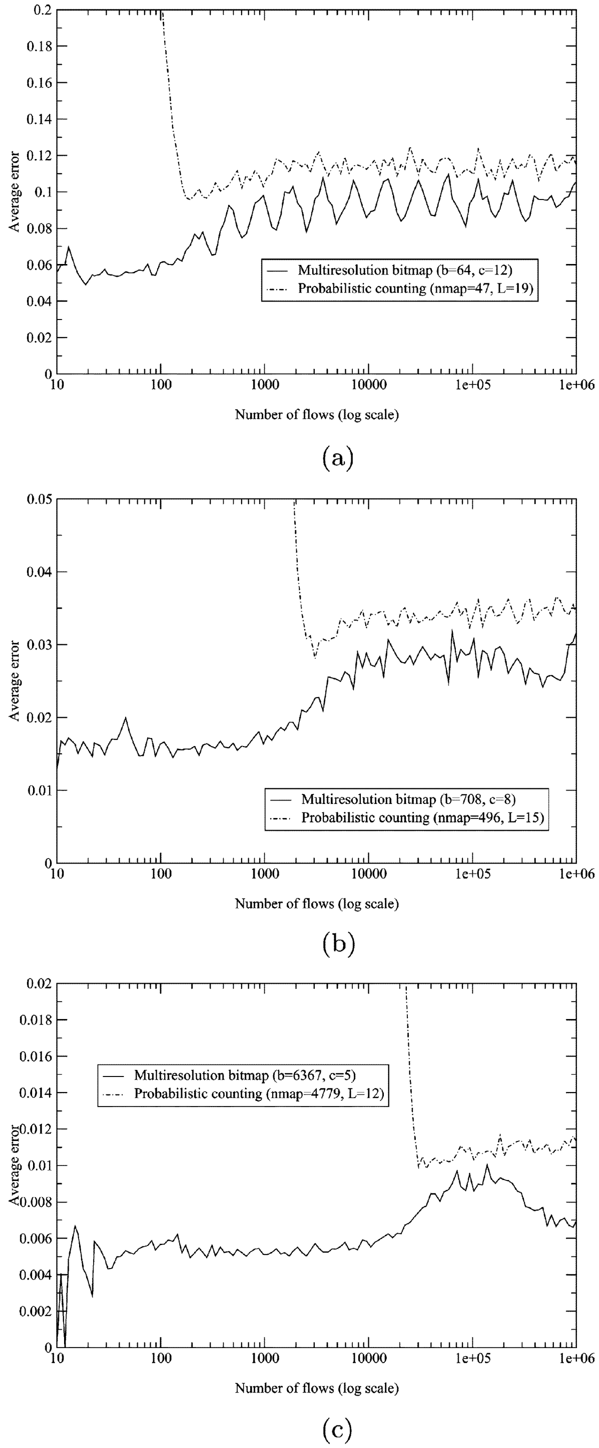

(a)

(b)

(c)

Fig. 6. Comparing multiresolution bitmap and probabilistic counting. (a) Configured for an average error of 10%. (b) Configured for an average error of 3%. (c) Configured for an average error of 1%.

TABLE V
COMPARISON OF ADAPTIVE BITMAP AND PROBABILISTIC COUNTING, EACH USING 16 kb OF MEMORY

Trace	Adaptive bitmap (min/avg/max)	Probabilistic counting (min/avg/max)
MAG+	-4.402/1.066/4.717%	-9.525/2.820/13.262%
COS	-1.879/0.748/1.950%	-6.946/2.759/7.621%
IND	-1.767/0.601/1.772%	2.400/10.214/17.724%

The algorithms were configured to give the best possible average error and work up to 100 000 000 flows. For the adaptive bitmap, we used as a base a multiresolution bitmap with an average error of 10% with $k = 2, b = 64, c = 19$, and $b_{\text{last}} = 169$. The virtual bitmap component is 15, 063 bits large and replaces nine components of the multiresolution bitmap. For the adaptive bitmap, we did not include in our computations the first measurement interval when the adaptive bitmap was not tuned to the traffic. For the probabilistic counting, we used $nmap = 744$ bitmaps of $L = 22$ bits each. Adaptive bitmap is roughly three times more accurate than probabilistic counting. For the IND trace, which has a very small number of active flows, probabilistic counting has very bad error and is actually biased towards overestimating. This is the same as the problem we noticed in the previous section. The major message here is that an adaptive bitmap can achieve almost the same benefits of virtual bitmap (e.g., order of magnitude reduction in memory for same accuracy) when the number of flows does not vary dramatically.

D. Triggered Bitmap

So far, all of our measurements have focused on one instance of the counting problem to be used as a building block for solving more complex problems. The experiments from this section give a better image of how our algorithms can affect the resource consumption of an entire system.

We first address port scan detection that uses a large number (one per source) of instances of the counting problem multiplying the impact of any memory our algorithm can save. We use a definition of a port scan equivalent to the definition in the default Snort configuration: a source is flagged as a port scanner if it has at least four connections in a 12-s measurement interval. In the second experiment, we extend the measurement interval to 10 min to evaluate the algorithms against this more demanding definition. We ignore many of the details of the operation of Snort (e.g., reliance on TCP flags to classify connections) and concentrate on the core task of counting connections.

For the triggered bitmap we chose a configuration that is convenient to implement on a 32-bit machine: a direct bitmap of 4 B and a multiresolution bitmap with 11 components of 4 B each (except the last one, which is 8 B). The multiresolution bitmap is allocated after 8 bits are set in the direct bitmap. By our analysis, the multiresolution bitmap should ensure an average error of at most 14.1% for up to 43 817 connections and at most 15.5% for up to 175 269 connections.

We used two configurations, one with a 12-s prefix and one with a 600-s prefix of the MAG+ trace. For each configuration, we had 20 runs of with the triggered bitmap algorithm, using different random hash functions. The average of the error for flows that had at least four connections was 13.6%.[7] Our algorithm reported 84.6% of the sources with four connections as reaching the threshold, 98.1% of those with five, and all (100%) of the sources that had at least eight connections. In Table VI, we

[7] This is an average over all sources. We did notice some "peculiarities": for sources that had four connections, the average error was around 10.5%, for those with five connections around 11%, for those with six connections it was 18%, for those with eight it was around 11.5%, while for all others the averages were roughly in the range 14%–15.5%. We explain these as effects of having such a small direct bitmap.

TABLE VI
MEMORY USAGE OF PORT SCAN DETECTION ALGORITHMS (kB)

Measurement interval	Snort	Prob. count.	Triggered bmp.
12 sec	1,968K	2,474K	381K
600 sec	50,791K	22,876K	5,725K

report the *maximum* of triggered bitmap over the 20 runs. Triggered bitmap uses roughly five times less memory than Snort with the first configuration. For the more ambitious second configuration the gain increases to a factor of nine. In both cases, triggered bitmap used less memory than probabilistic counting.

What do these results mean to a security analyst? Snort, of course, uses the classical measure of detecting n connections with a maximum inter-event spacing of t. By default, Snort uses values such as $n = 4$ and $t = 3$. Our technique uses significantly less memory at the expense of possibly missing port scanners. However, the probability of a port scanner not being detected decreases exponentially with the number of connections it opens. For example, the probability is 1.87% at five connections, 0.23% at six, 0.03% at seven, and so on. Using Snort's timing requirements, a fifth event must arrive within $t = 3$ seconds of the fourth event if the scan continues. Thus, we detect a continuing scan with probability 98.13% within 3 s and 99.77% within 6 s. Note also that port scans are usually the result of a brute-force network exploration such as Nmap [9] or Code Red [15]. Such tools frequently touch not just a handful of addresses, but an entire block of contiguous addresses.

Finally, note that because our algorithms reduce the memory usage by as much as an order of magnitude, they also enable detection of stealthy slow scans using the same amount of memory that naive algorithms use for fast scans. Because the memory required for each source is greatly reduced with our algorithms, we can afford to count more sources at a time. We can avoid timing-out state as aggressively as Snort and keep counting sources with longer inter-arrival times between events. Finding these more stealthy port scans is a goal of many detection systems [20].

VI. CONCLUSION

Using a suitably general definition of a flow, counting the number of active flows is at the core of a wide variety of security and networking applications such as detecting port scans and denial of service attacks, tracking worm infections, calibrating and caching. In this paper, we provide a family of bitmap algorithms solving the flow counting problem using extremely small amounts of memory. Most of the algorithms can be implemented at wire speeds (8 ns per packet for OC-768) using SRAM since they access at most one memory location per packet and can be implemented using simple hardware (CRC-based hash functions, multipliers, and multiplexers). With the exception of direct and virtual bitmap, the other algorithms are introduced for the first time in this paper.

TABLE VII
FAMILY OF BITMAP COUNTING ALGORITHMS: EACH ALGORITHM IS BEST SUITED FOR A DIFFERENT SETTING

Setting	Algorithm	Application
General counting	Multiresolution bitmap	Tracking worm infections
Accuracy important only over a narrow range	Virtual bitmap	Triggers (e.g. for detecting DoS attacks)
Count is probably in a narrow range (stationarity)	Adaptive bitmap	Measurement
Small memory usage as long as count is small	Triggered bitmap	Detecting port scans

The most popular algorithm for counting distinct values is probabilistic counting. Our algorithms need less memory to produce results of the same accuracy. This translates into savings of scarce, fast memory (SRAM) for hardware implementations. It also helps systems that use cheaper DRAM to scale to larger instances of the problem.

In comparing head on with probabilistic counting, our multiresolution algorithm works under the same assumptions and provides an error orders of magnitude lower when the number of flows is small and is slightly better for higher values. However, we believe our biggest contribution is as follows. By exposing the simple building blocks and analysis behind multiresolution counting, we have provided a family of *customizable* counting algorithms (Table VII) that application and hardware designers can use to reduce memory even further by exploiting application characteristics.

Thus, virtual bitmap is well-suited for triggers such as detecting DoS attacks and uses 215 bytes to achieve an error of 2.773% compared with 2076 B for probabilistic counting. Adaptive bitmap is suited to flow measurement applications and exploits stationarity to require eight times less memory than probabilistic counting on sample traces. Triggered bitmap is suited to running multiple instances of counting where many instances have small count values (e.g., port scanning) requiring only 5.6 MB on a 10-min trace compared with the 49.6 MB required by the naive algorithm and 22.3 MB required by probabilistic counting. Using triggered bitmap resulted in a reduction by 29% in the running time and a factor of seven in the total memory usage of a traffic analysis application from the CoralReef suite. Given that low-memory counting appears to be useful in applications beyond networking which have different characteristics, we hope that the base algorithms in this paper will be combined in other interesting ways in architecture, operating systems, and even databases.

APPENDIX A
HARDWARE IMPLEMENTATION OF THE MULTIRESOLUTION BITMAP

The implementation of multiresolution bitmap is much simpler than its analysis. The most time critical per packet part of the algorithm is updating the bitmap. The hash function on the flow IDs can be implemented with combinatorial logic that is easy to pipeline. Computing the address of the bit to get updated is also quite simple in hardware if three constraints are met: ratio of the resolutions of neighboring components k, the size of the last component and $bk/(k-1)$ need to be powers of two. Thus, for the multiresolution bitmap example in Fig. 2 ($b = 6$, $k = 4$), one can map the incoming packets to the proper subinterval by computing a 7-bit hash function and using simple additional combinatorial logic. If the first two bits of the hash are not "11," the first 3 bits decide which of the subintervals in the coarsest component the packet maps to. Otherwise, if the third

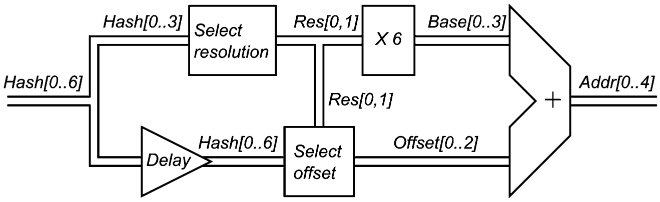

Fig. 7. Hardware for selecting the bit to be set.

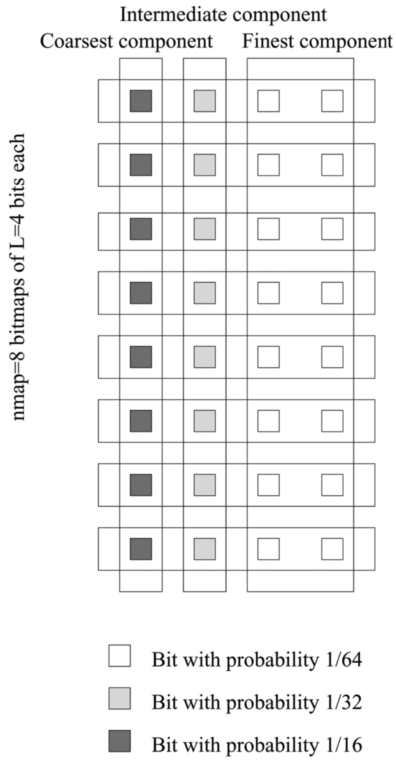
Intermediate component
Coarsest component
Finest component
nmap=8 bitmaps of L=4 bits each
□ Bit with probability 1/64
▨ Bit with probability 1/32
■ Bit with probability 1/16

Fig. 8. Probabilistic counting groups bits horizontally, so bitmaps have bits with different probabilities of being set. Multiresolution bitmaps group bits vertically so components have bits with the same probability of being set.

and fourth bit are not 11 (but the first two are), bits from 3 to 5 decide which subinterval in the intermediate component the packet maps to. If the first 4 bits are 1, bits from 5 to 7 map the packet to the appropriate subinterval in the finest component.

Fig. 7 presents a possible hardware implementation for the logic circuit that computes the address of the bit the current packet maps to. The input to the circuit is the 7-bit hash function $\mathrm{Hash}[0..6]$ that is based on the flow ID of the packet. Its output is a 5-bit address $\mathrm{Addr}[0..4]$ of the bit that will be set. The leftmost bit in the multiresolution bitmap of Fig. 2 has an address of 0 and the rightmost has an address of 19. The "select resolution" block selects the component with the appropriate resolution based on the first 4 bits of the hash. If the coarsest component is used, the output $\mathrm{Res}[0,1]$ will have a value of 0 and if the finest component is used its value will be 2. This block can be implemented with few gates. The "X 6" block multiplies this value by 6 and it can be implemented using an adder and a shift register. The "Select offset" block selects which of the bits within the hash to use to find the offset of the bit within the component. It can be implemented with a 16:4 multiplexer. The final adder adds the base and the offset to get the bit's address.

Appendix B
Multiresolution Bitmap Versus Probabilistic Counting

Even though it might seem surprising at first, the data collected by a multiresolution bitmap with $k=2$ and no stretching of the last component ($b_{last} = bk/(k-1)$) are statistically equivalent to the data collected by a matching configuration of the probabilistic counting algorithm (under the assumption of perfect hash functions). The probability of the incoming packet to hash to component i is $1/2^i$ for all components but the last for which it is $1/2^{c-1}$. Each component but the last has b bits.

The probability that the packet hashes to a given bit at component i is $1/2^i * 1/b = 1/(b*2^i)$ (this also holds for the last component). Therefore, for each i from 1 to $c-1$, we have b bits that have a probability of $1/(b*2^i)$ of "catching" the incoming packet, plus we have $2b$ bits that have the probability $1/(b*2^c)$ of "catching" the incoming packet. All incoming packets map to exactly one bit.

Probabilistic counting of Flajolet and Martin uses $nmap$ bitmaps of size L. Each bitmap has a probability of $1/nmap$ of "catching" a random database record. Within each bitmap, bit i has a probability of $1/2^i$ of catching the record. The last bit acts as a "catch-all" for all numbers of consecutive zeroes of L or more in the hash, so it has a probability of $1/2^{L-1}$ of catching the packet. Overall, for each i from 1 to $L-2$, we have $nmap$ bits that have a probability of $1/(nmap*2^i)$ of "catching" the record plus, we have $2*nmap$ bits that have a probability of $1/(nmap*2^{L-1})$ of "catching" the record.

We can see in Fig. 8 that, when $b = nmap$ and $c = L-1$, the two algorithms have the same number of bits and the probability distribution of bits getting set is the same. Thus, the data collected by the two algorithms is statistically equivalent. However, there is a significant difference in the accuracy of their estimates (see Section V-B) because of the way the data are interpreted. As both analysis and experiments show, this leads to our algorithm being more accurate when the number of flows is small. Another difference is that we have tighter rules for configuring the algorithm which result in somewhat more accurate experimental results when the number of flows is large.

Acknowledgment

The authors would like to thank V. Paxson, D. Moore, P. Flajolet, M. Durand, A. Snoeren, K. Claffy, S. Savage, and F. Baboescu for extremely valuable conversations.

References

[1] Cisco Offers Wire-Speed Intrusion Detection. 2000 [Online]. Available: http://www.nwfusion.com/reviews/2000/1218rev2.html

[2] N. Duffield, C. Lund, and M. Thorup, "Properties and prediction of flow statistics from sampled packet streams," presented at the SIGCOMM Internet Measurement Workshop, Marseille, France, Nov. 2002.

[3] C. Estan, The bmpcount library of flow counting algorithms. [Online]. Available: http://ial.ucsd.edu/bitmaps/

[4] C. Estan and G. Varghese, "New directions in traffic measurement and accounting," presented at the ACM SIGCOMM, Pittsburgh, PA, Aug. 2002.

[5] C. Estan, G. Varghese, and M. Fisk, "Bitmap algorithms for counting active flows on high speed links," in *Internet Measurement Conf. (IMC'03)*, Miami Beach, FL, Oct. 2003.

[6] ——, Bitmap algorithms for counting active flows on high speed links Comput. Sci. Eng. Dept., Univ. California, San Diego, Tech. Rep. 0738, 2003.

[7] W. Fang and L. Peterson, "Inter-as traffic patterns and their implications," in *Proc. IEEE GLOBECOM*, Dec. 1999, vol. 3, pp. 1859–1868.

[8] P. Flajolet and G. N. Martin, "Probabilistic counting algorithms for data base applications," *J. Comput. Syst. Sci.*, vol. 31, no. 2, pp. 182–209, Oct. 1985.

[9] Fyodor, "Remote OS detection via TCP/IP stack fingerprinting," *Phrack*, vol. 54, Dec. 1998.

[10] K. Keys, D. Moore, and C. Estan, "A robust system for accurate real-time summaries of internet traffic," presented at the ACM SIGMETRICS Conf., Banff, Canada, Jun. 2005.

[11] K. Keys, D. Moore, R. Koga, E. Lagache, M. Tesch, and K. Claffy, "The architecture of Coralreef: An internet traffic monitoring software suite," presented at the Workshop on Passive and Active Measurements (PAM2001), Amsterdam, The Netherlands, Apr. 2001.

[12] A. Kumar, J. Xu, J. Wang, O. Spatschek, and L. Li, "Space-code Bloom filter for efficient per-flow traffic measurement," in *Proc. IEEE INFOCOM*, Mar. 2004, pp. 1762–1773.

[13] R. Mahajan, S. M. Bellovin, S. Floyd, J. Ioannidis, V. Paxson, and S. Shenker, "Controlling high bandwidth aggregates in the network," in *Proc. ACM SIGCOMM*, Jul. 2002, pp. 62–73.

[14] M. Durand and P. Flajolet, "Loglog counting of large cardinalities," presented at the Eur. Symp. Algorithms (ESA), Budapest, Hungary, Sep. 2003.

[15] CAIDA analysis of Code Red. 2001 [Online]. Available: http://www.caida.org/analysis/security/code-red/

[16] Cisco Netflow. [Online]. Available: http://www.cisco.com/warp/public/732/Tech/netflow

[17] LFAP: Lightweight Flow Accounting Protocol, Riverstone Networks. [Online]. Available: http://www.riverstonenet.com/ technology/accounting_for_profitability.shtml

[18] D. Plonka, "Flowscan: A network traffic flow reporting and visualization tool," in *Proc. 14th Systems Administration Conf., USENIX LISA*, New Orleans, LA, Dec. 2000, pp. 305–317.

[19] M. Roesch, "Snort: Lightweight intrusion detection for networks," in *Proc. 13th Systems Administration Conf., USENIX LISA*, Seattle, WA, 1999, pp. 229–238.

[20] S. Staniford, J. Hoagland, and J. McAlerney, "Practical automated detection of stealthy portscans," *J. Comput. Security*, vol. 10, no. 1–2, pp. 105–136, 2002.

[21] S. Venkataraman, D. Song, P. B. Gibbons, and A. Blum, "New streaming algorithms for fast detection of superspreaders," presented at the Network and Distributed Systems Symp. (NDSS), San Diego, CA, Feb. 2005.

[22] K.-Y. Whang, B. T. Vander-Zanden, and H. M. Taylor, "A linear-time probabilistic counting algorithm for database applications," *ACM Trans. Database Syst.*, vol. 15, no. 2, pp. 208–229, 1990.

Cristian Estan received the B.Sc. and M.Sc. degrees from the Technical University of Cluj-Napoca, Cluj-Napoca, Romania, and the Ph.D. degree from the University of California at San Diego, in 2003.

Since 2004, he has been an Assistant Professor of computer science with the University of Wisconsin-Madison, where his research focuses on tools for measurement and analysis of the traffic of IP networks.

Prof. Estan has been a member of the Association for Computing Machinery since 2002.

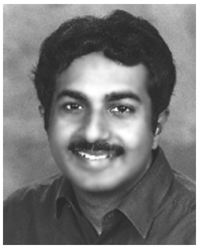

George Varghese (M'99) received the Ph.D. degree from the Massachusetts Institute of Technology, Cambridge, in 1992.

He was with DEC for several years designing DECNET protocols before completing his doctoral work. After working from 1993 to 1999 with Washington University, St. Louis, MO, he joined the University of California at San Diego, where he currently is a Professor of computer science. He works on efficient protocol implementation and protocol design. Together with colleagues, he has 12 awarded and several pending patents. Several of the algorithms he has helped develop (e.g., IP Lookups, timing wheels, DRR) have found their way into commercial systems. He is the author of the textbook *Network Algorithmics* (Morgan-Kaufman, 2004).

Prof. Varghese has been a Fellow of the Association for Computing Machinery since 1999. He was the recipient of the Office of Naval Research Young Investigator Award in 1996.

Michael Fisk received the B.S. degree in computer science from the New Mexico Institute of Mining and Technology, Socorro, in 1996, and the M.S. degree in computer science from the University of California at San Diego (UCSD), in 2001. He is currently working toward the Ph.D. degree in computer science at UCSD.

He is a Technical Staff Member with the Network Group, Los Alamos National Laboratory, Los Alamos, NM, and an Adjunct Staff Researcher with the Center for Computing Sciences, Bowie, MD. His focus is network measurement and traffic analysis for security applications and continuous relational query systems.